Inelastic neutron scattering study of the rotational excitations in (KBr)1−x(KCN)x in the paraelastic and structural glass state

Alois Loidl, R. Feile, K. Knorr, J. K. Kjems

Angaben zur Veröffentlichung / Publication details:

Loidl, Alois, R. Feile, K. Knorr, and J. K. Kjems. 1984. "Inelastic neutron scattering study of the rotational excitations in (KBr)1−x(KCN)x in the paraelastic and structural glass state." *Physical Review B* 29 (11): 6052–62. https://doi.org/10.1103/physrevb.29.6052.

Inelastic neutron scattering study of the rotational excitations in $(KBr)_{1-x}(KCN)_x$ in the paraelastic and structural glass state

A. Loidl
Institut für Physik, Johannes Gutenberg Universität Mainz, D-6500 Mainz, West Germany

R. Feile
Institut für Physik, Johannes Gutenberg Universität Mainz, D-6500 Mainz, West Germany and Risø National Laboratory, DK-4000 Roskilde, Denmark

K. Knorr
Institut für Physik, Johannes Gutenberg Universität Mainz, D-6500 Mainz, West Germany

J. K. Kjems
Risø National Laboratory, DK-4000 Roskilde, Denmark
(Received 15 November 1983)

The coupled rotational-translational excitations in $(KBr)_{1-x}(KCN)_x$ were studied by inelastic neutron scattering for concentrations $0.008 \leq x \leq 0.20$. We followed the A_{1g}-T_{2g} tunneling transition and the A_{1g}-E_g librational excitation through the transition from the paraelastic to the structural glass state. We found that these two excitations and their coupling to the lattice strains exhibit a very different temperature dependence in the glass state. While the tunneling transition, which triggers reorientations of the CN^- ions, shows a drastic reduction of the T_{2g} rotation-translation coupling, the librational excitations conserving the CN alignment are less influenced. These results suggest that for $T \leq T_F$ the CN system is gradually blocked in clusters, thereby reducing the density of free-ion tunneling states in favor of cluster-reorientation modes effectively decoupled from the lattice. This leads to a metastable low-temperature state with extremely long relaxation times.

I. INTRODUCTION

Neutron scattering is an ideal tool for studying the reorientational and librational motions of aspherical molecules in an effective potential built up by the surrounding ions in the crystal. Generally, the molecules can have several equilibrium orientations which are determined by the minima of the orientational potential. The molecular dynamics is characterized by two extreme cases: When the temperatures are high compared to the potential barriers one has a relaxational regime, a situation of rotational diffusion; when the temperature is low the molecules are caught in high hindering potentials, and libration and quantum-mechanical tunneling can be observed.

In $(KBr)_{1-x}(KCN)_x$ mixed crystals both limiting cases can be found. At very low concentrations ($x \ll 0.01$) tunneling transitions have been measured with optical experiments,[1,2] paraelastic resonance,[3] monochromatic phonon spectroscopy,[4] and neutron inelastic scattering techniques.[5] In pure KCN, a relaxational model accounts for the measured line shapes in the inelastic neutron scattering experiments.[6,7] Many experimental efforts have been undertaken to measure the rotational-level scheme for the entire range of CN concentrations. The most successful studies were performed by inelastic neutron scattering where the molecular excitations were probed via their hybridization with phonons of certain symmetry. The pioneering work was performed by Walton *et al.*[8] In $KCl_{0.996}KCN_{0.004}$ they observed a librational excitation from an A_{1g} rotational ground state to an excited E_g state at an energy of 1.8 meV. Later,[9] these investigations were extended to $(KCl)_{1-x}(KCN)_x$ crystals with concentrations x ranging from $0.004 \leq x \leq 0.06$. The results for $x \leq 0.02$ were well described theoretically by Woods and Mostoller[10] in terms of a single rotational excitation coupled to acoustic phonons. For higher concentrations this simple model failed to describe the experimental findings correctly.[9] Analogous experiments were carried out in $(KBr)_{1-x}(KCN)_x$ for concentrations $x = 0.005$,[5] 0.035, and 0.16.[11] Here, the A_{1g}-E_g librational energy was found to depend strongly on x, rising from 1.6 meV at $x = 0.005$ to 4 meV at $x = 0.16$. This shift of the lowest E_g-symmetry molecular excitation was also observed in Raman experiments in $(KCl)_{1-x}(KCN)_x$ and $(KBr)_{1-x}(KCN)_x$.[2,12] In T_{2g} symmetry a tunneling transition at 0.28 meV was observed in $(KBr)_{1-x}(KCN)_x$ ($x = 0.000\,34$) by inelastic neutron scattering.[5] For concentrations of $x = 0.16$, a relaxational behavior accounts for the measured neutron line shapes.[11] Surprisingly, the coupling strength was found to be weaker at lower temperatures, which contradicts the simple mode-coupling model between phonons and a single molecular excitation.[10]

The present study was motivated by the increasing experimental[13–20] and theoretical[21–23] evidence that a glass-like phase exists in $(KBr)_{1-x}(KCN)_x$ for concentrations x less than 0.56.[12,14] This structural glass state is characterized by a short-range order of the frozen-in CN^- ions, as suggested by the pattern of quasielastic, diffuse scattered intensities in neutron experiments.[13,21] Its occurrence was

first predicted by Fischer and Klein[22] and it is thought to result from a frustration of the effective multipole interactions between CN^- ions into which not only the orientation of the multipoles but also the bond vectors enter. The cusps of the temperature-dependent electric dipolar[15,16,19] and quadrupolar[13–15,17,18] susceptibilities were regarded as signals for the onset of the structural glass state at the freezing temperature T_F. The electric dipolar susceptibility is measured directly in dielectric measurements, while the quadrupolar one has been determined via the coupling to long-wavelength phonons in ultrasonic, Brillouin, and inelastic neutron scattering experiments. The freezing temperatures exhibit a strong frequency dependence, demonstrating that the glass state is a nonequilibrium phenomenon.[15,16]

In this paper we report a systematic inelastic neutron scattering study on coupled phonon-rotational excitation modes in $(KBr)_{1-x}(KCN)_x$ for concentrations in the range $0.008 \leq x \leq 0.20$. In particular, we address our attention to the dynamics of the molecular excitation at the transition from the paraelastic to the structural glass state, which gives us direct insight into the glass-formation process.

II. THEORETICAL PREDICTIONS

Devonshire[24] has calculated the energy levels of a hindered rotator assuming a cubic hindering potential of lowest-order spherical harmonics. This model has been extended by Beyeler[25] to include cubic fields in terms of linear contributions of the spherical harmonics V_4 and V_6 of order 4 and 6, respectively. The potential used had the form

$$V = K(V_4 \cos\phi + V_6 \sin\phi) . \tag{1}$$

The parameter K measures the intensity of the potential, whereas the mixing angle ϕ determines its shape. The results for $\phi = 225°$ and $K = 4$ meV are shown in Fig. 1. This potential yields the $\langle 111 \rangle$-oriented ground state which describes the experimental situation in $(KBr)_{1-x}(KCN)_x$.[2] The parameters K and ϕ were chosen to fit the molecular excitations which were found in mixed crystals with very low concentrations x.[1,12] The arrows indicate quadrupolar transitions in E_g and T_{2g} symmetry which are strongly coupled to the phonons and have been verified experimentally.[5,9]

The interaction of rotational excitations with the normal modes of the host crystal were studied theoretically by several authors,[26,27,6,10] with the main result that a coherent mixed-mode state of rotational and translational excitations exists.

In the analysis of our experimental data we follow the pseudospin approach of Silverman,[28] which yields a mixed-mode behavior ($\Delta \gg \Gamma$) as well as the relaxational behavior as limiting cases. This model was used to calculate the coupled proton-phonon system potassium dihydrogen phosphate (KDP).[28] However, similar pseudospin theories have been used to account for phase transitions in Jahn-Teller systems and in a variety of molecular crystals where the spin variable specifies the orientational configuration of the aspherical ions.[29]

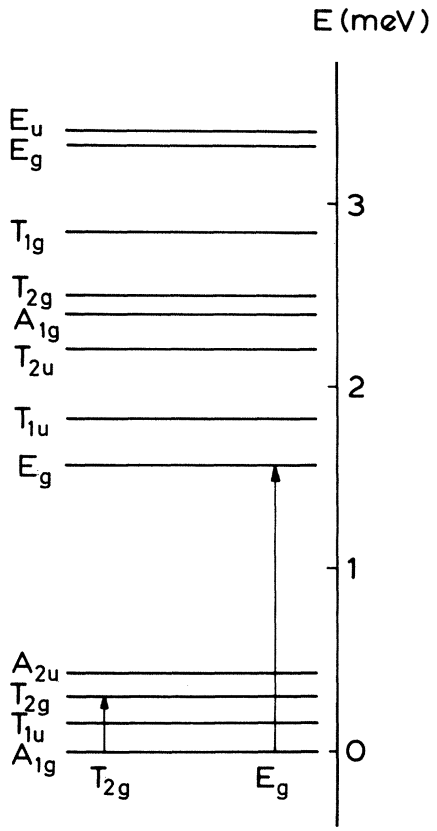

FIG. 1. Approximate level scheme of a rigid CN dumbbell in an octahedral hindering potential of KBr (Ref. 12). The arrows indicate librational (E_g) and tunneling (T_{2g}) excitations which couple to the phonons.

Assuming a two-level system, the molecular susceptibility can be written as

$$\chi(\omega) = \frac{2}{\hbar\Delta} \tanh\left[\frac{\hbar\Delta}{2k_B T}\right] \frac{\Delta^2+\Gamma^2+i\omega\Gamma}{\Delta^2+\Gamma^2-\omega^2+2i\omega\Gamma} , \tag{2}$$

with the level separation Δ and linewidth Γ. Equation (2) neglects the interaction between the "spins."

The phonon propagator in this coupled pseudospin-phonon system is given by[28]

$$D(\vec{q},\omega) = \frac{2\omega_0(\vec{q})}{\omega^2(\vec{q}) - \omega^2 - xG^2(\vec{q})\chi(\omega) + i\gamma\omega} . \tag{3}$$

$\omega_0(\vec{q})$ is the undisturbed "bare" phonon frequency and $G^2(\vec{q})$ is the rotational-translational coupling constant. For small wave vectors $G(\vec{q})$ is proportional to $\vec{q}$, and γ is an additional damping constant due to phonon-phonon interactions. The dynamic structure factor yields the shape of the scattered-neutron groups. It is given by

$$S(\vec{q},\omega) = [1 - \exp(-\beta\omega)]^{-1} \mathrm{Im} D(\vec{q},\omega) . \tag{4}$$

For $\Gamma \ll \Delta$ this analysis is very similar to the mixed-mode behavior used by Wood and Mostoller[10] and by Casella.[26] However, for $\Gamma > \Delta$ the molecular susceptibility of Eq. (1) can be written as

$$\chi(\omega)=\frac{2}{\hbar\Delta}\tanh\left[\frac{\hbar\Delta}{2k_BT}\right]\frac{\Gamma}{\Gamma+i\omega}\ . \tag{5}$$

In a high-temperature limit $k_BT\gg\hbar\Delta$ this reduces to the well-known relaxational susceptibility

$$\chi(\omega)=\frac{1}{k_BT}\frac{1}{1+i\omega\tau}\ , \tag{6}$$

with the relaxation time $\tau=1/\Gamma$. A similar molecular susceptibility was used in the analysis of neutron line shapes in pure KCN.[6]

III. EXPERIMENTAL DETAILS

The four samples investigated were single crystals obtained from the crystal-growth laboratory of the University of Utah. They were grown from the melt using zone-refined KBr and KCN as starting material. A determination of the densities and the infrared absorption yielded CN concentrations x of 0.008, 0.035, 0.16, and 0.20. These figures differ from the nominal concentrations of the melt, which have been 0.01, 0.05, 0.20, and 0.25, respectively, and also from the results of a chemical analysis. Based on chemical analyses, concentrations of 0.04 and 0.14 were cited for the second and third sample, respectively, in our previous work.[11,14,15]

The neutron experiments were performed on the triple-axis spectrometers TAS6 and TAS7 located at the cold source of the DR3 reactor of the Risø National Laboratory. All scans were performed in the (001) scattering plane with the constant-$\vec{Q}$ mode of operation. Depending on the needs of momentum and energy resolution, the incident or the outgoing energy was held constant between 2.5 and 5 meV, or at 14.7 meV. In order to avoid higher-order contaminations a liquid-nitrogen–cooled beryllium filter or a pyrolytic graphite filter was used, respectively. A typical collimation was 30′ both before and after the monochromator and analyzer crystals.

IV. EXPERIMENTAL RESULTS

A. Determination of the freezing temperatures

The transition temperatures from the paraelastic to the structural glass state are identified as those temperatures where (i) the long-wavelength phonons have the lowest energies for fixed wavevectors q/q_{zB}, and (ii) the quasielastic scattering around the Bragg points sets in, signaling the onset of short-range orientational order of the frozen-in CN^- ions. We present some of the raw data for $(KBr)_{0.84}(KCN)_{0.16}$ in Fig. 2. A summary of these measurements is shown by the temperature dependence of the phonon energy and of the quasielastic scattered intensities of all the scans along [1,0,0] T_y (the subscript characterizes the direction of the phonon polarization vector) in Fig. 3. At about 55 K the slope of the dispersion near the zone center goes through a minimum, and with further decreasing temperatures the quasielastic scattering increases significantly. The scattered neutron groups are well defined even at T_F, although there is some additional line broadening just below the freezing temperature.

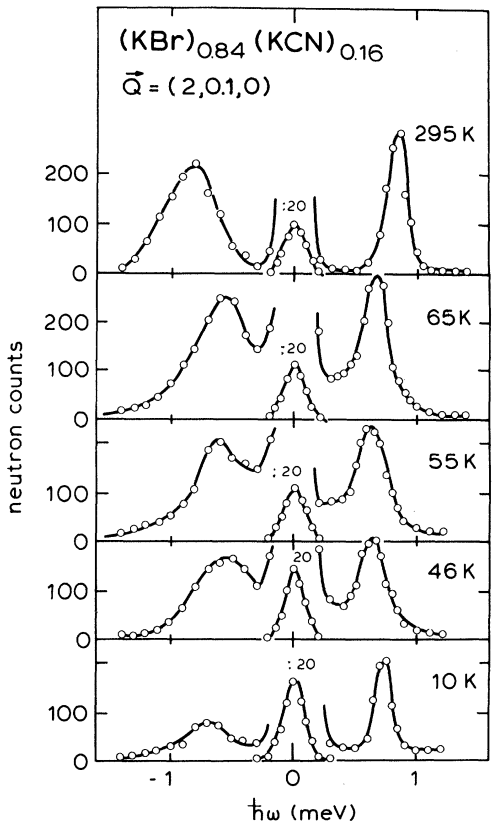

FIG. 2. Neutron-scattering line shapes in T_{2g} symmetry for different temperatures. The solid lines are guides to the eye.

Similar results were obtained in a crystal with a CN concentration $x=0.20$. In $(KBr)_{0.992}(KCN)_{0.008}$ no softening of the phonon frequencies as function of temperature could be observed at $\vec{Q}=(2,0.1,0)$, but a very slight increase of quasielastic scattered intensities could be detected below 9 K which saturates at 2.5 K with an extra

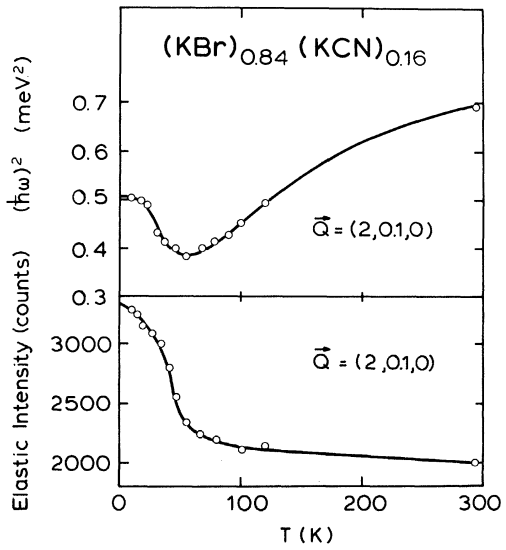

FIG. 3. Squared phonon frequency and the elastic intensity at $\vec{Q}=(2,0.1,0)$ versus temperature, displaying the freezing process in the $x=0.14$ mixed crystal.

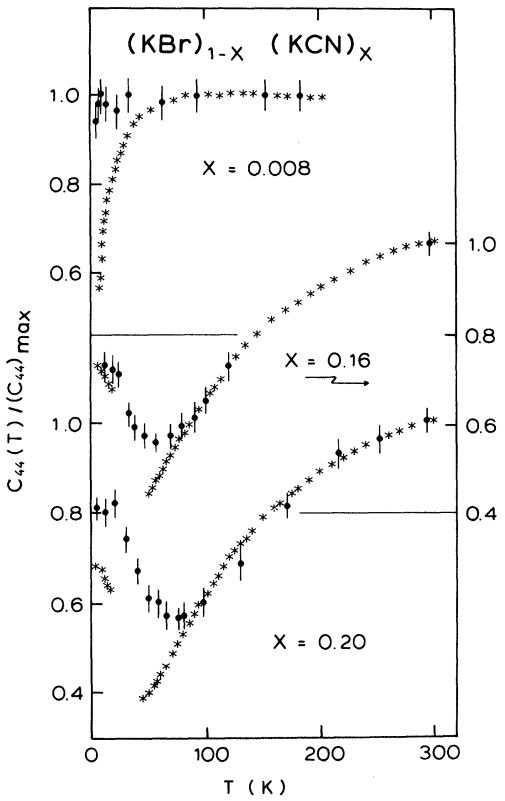

FIG. 4. Normalized elastic constant versus temperature for different concentrations, showing the deviation of the ultrasonic (*) from inelastic neutron scattering studies (●).

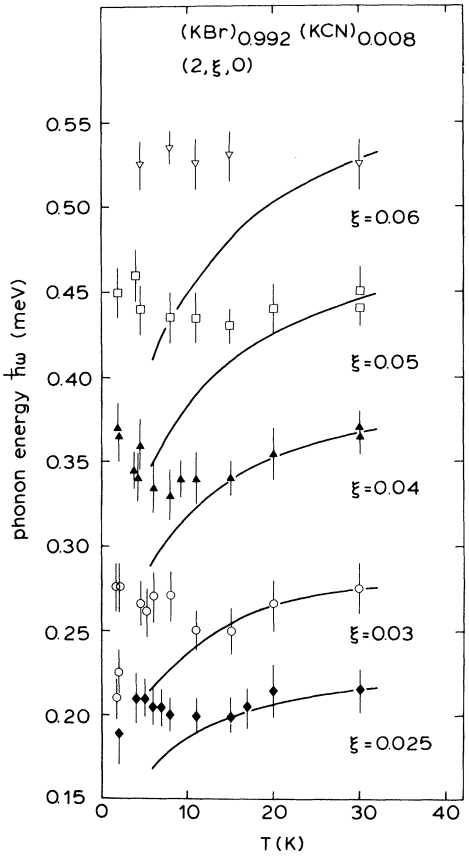

FIG. 5. Temperature dependence of the energies of transverse phonons of T_{2g} symmetry for various momentum transfers in comparison with scaled ultrasonic results (solid lines).

intensity of about 15% above the incoherent background. Figure 4 shows a comparison of the elastic constants c_{44} when measured by ultrasonic sound propagation and when determined from the centers of the inelastic scattered-neutron groups at a reduced wave vector $q/q_{zB}=0.1$. The neutron results agree well with the ultrasonic data at higher temperatures, but for $x=0.16$ and 0.20 the minima determined in the neutron-scattering experiments are more shallow and occur at higher temperatures. The largest discrepancy between the results for the two measuring frequencies was observed for the lowest concentration $x=0.008$, where the ultrasonic elastic constant shows a temperature variation of more than 40%; the neutron data are practically temperature independent. All of these data demonstrate the presently well-established effect of a strong frequency dependence of the freezing temperatures T_F. However, the measuring frequencies ω_{us} and ω_n for the ultrasonic and the neutron experiments, respectively, probe the slow relaxation regime for $x=0.16$ and 0.20, whereas for $x=0.008$, $\omega_n > 1/\tau > \omega_{us}$ is obeyed. A series of temperature-dependent scans with a constant momentum transfer at smaller wave vectors were performed to localize the transition region from fast-to-slow molecular relaxation in $(KBr)_{0.992}(KCN)_{0.008}$. Figure 5 shows the results. We find that the relation $\omega\tau=1$ is satisfied at approximately 0.40 meV. At lower frequencies a minimum at 10 K is well established. In Fig. 5 phonon energies as calculated from ultrasonic results assuming a linear dispersion relation are shown as solid lines. Table I summarizes the observed freezing temperatures measured at Thz and MHz frequencies. From these results we conclude that all the samples investigated show a transition into a metastable low-temperature state with a characteristic short-range-order pattern of frozen-in CN^- ions.

TABLE I. Freezing temperatures as measured with neutrons of THz frequencies and with ultrasonic techniques (Ref. 18) of MHz frequencies in $(KBr)_{1-x}(KCN)_x$. (nd denotes "not determined.")

x	T_F(10 MHz) (K)	T_F(~THz) (K)
0.008±0.001	4.0±0.2	10.0±2.0
0.035±0.003	16.5±0.5	nd
0.16 ±0.02	40.0±3.0	55.0±5.0
0.20 ±0.03	45.0±3.0	75.0±8.0

B. Coupled modes in E_g symmetry.

The results of the scans giving the [110] $T_{x\bar{y}}$ phonon branch in the mixed crystals are shown in Figs. 6—11. Here, we selected scans in the regions of energy and

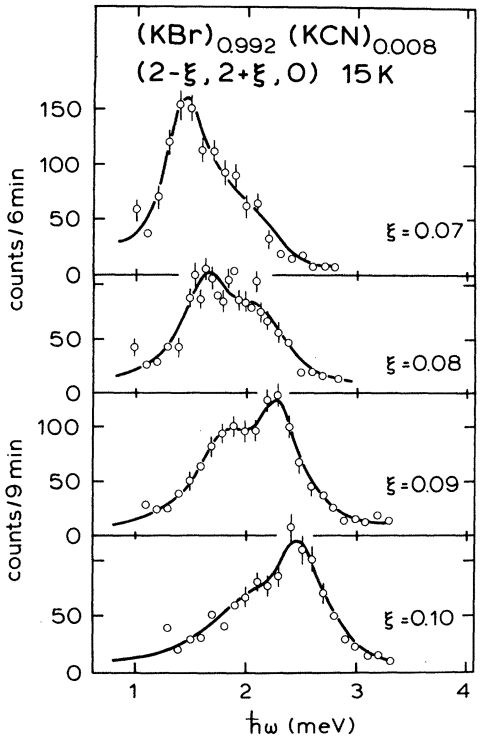

FIG. 6. Neutron-scattering line shapes in E_g symmetry at 15 K. The solid lines are calculated from the Silverman model.

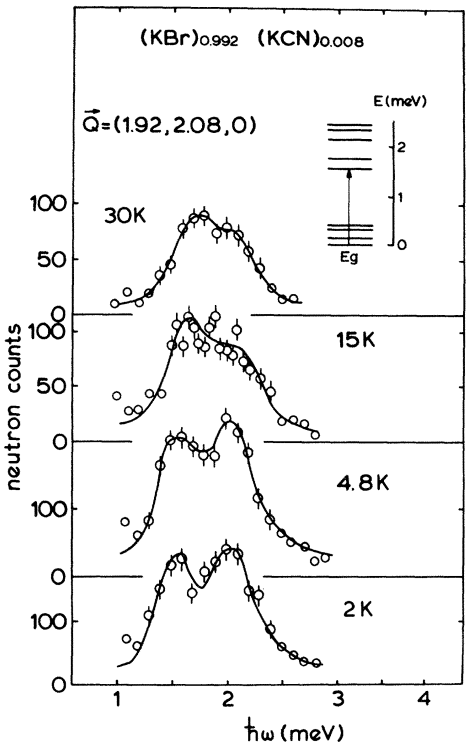

FIG. 8. Temperature dependence of the neutron-scattering line shape at constant momentum transfer in E_g symmetry in the $x=0.008$ sample.

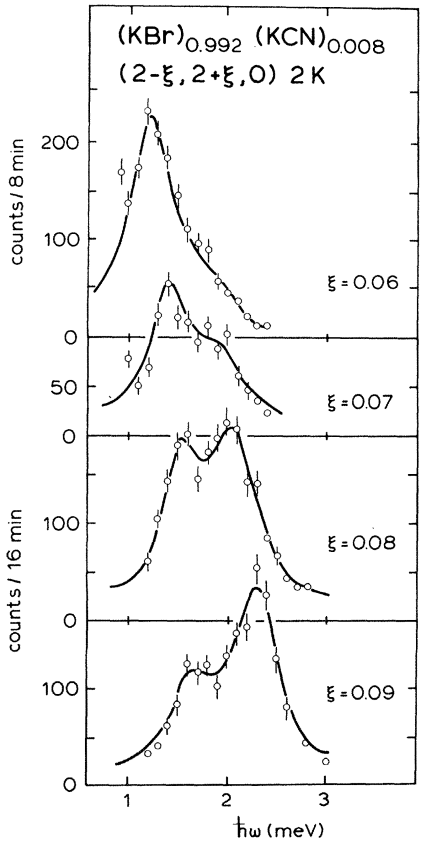

FIG. 7. Neutron-scattering line shapes in E_g symmetry at 2 K. The solid lines are calculated from the Silverman model.

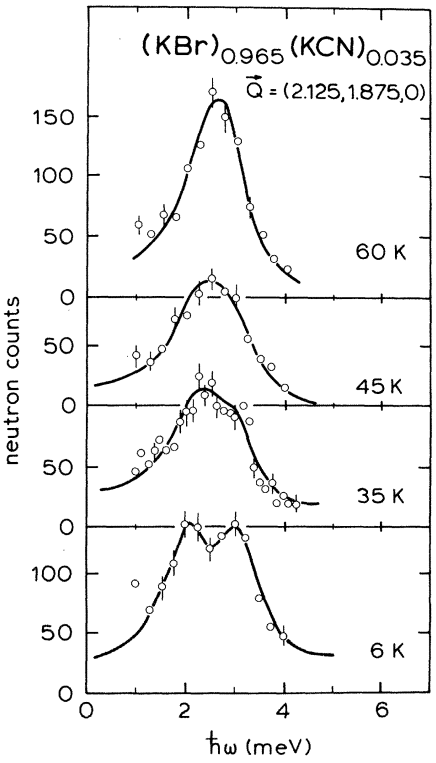

FIG. 9. Temperature dependence of the neutron-scattering line shapes at constant momentum transfer in E_g symmetry in the $x=0.035$ sample.

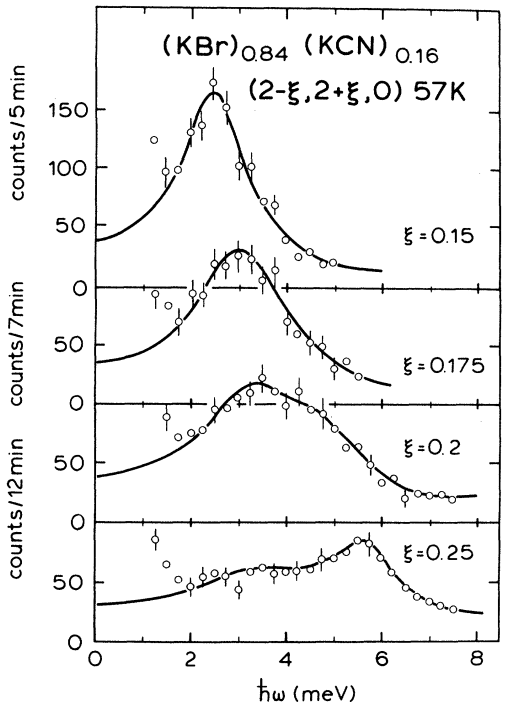

FIG. 10. Neutron-scattering line shapes in E_g symmetry for different momentum transfers at 57 K ($x=0.16$ sample).

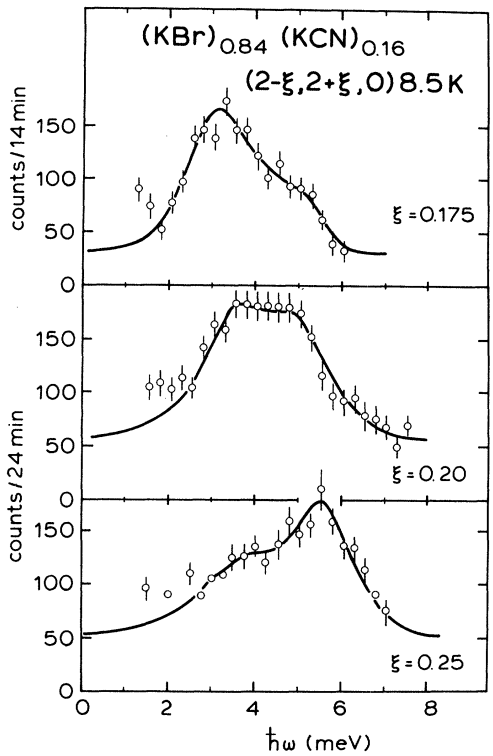

FIG. 11. Neutron-scattering line shapes in E_g symmetry for different momentum transfers at 8.5 K ($x=0.16$ sample).

momentum transfer where the interaction of the transverse phonons with rotational excitations is strongest. The hybridization effect is revealed by a double-peak structure in the scattered-neutron groups, which gives a direct measure of this interaction. Each crystal is represented by measurements at different temperatures covering the paraelastic ($T \geq T_F$) and the structural glass state ($T < T_F$). Figures 6 and 7 show constant-$\vec{Q}$ scans in the wave-vector region of the strongest rotation-translation coupling in both states in $(KBr)_{0.992}(KCN)_{0.008}$. The resonance energy is somewhat below 2 meV and is unaffected by the freezing process. Figure 8, showing the temperature dependence of the scattered-neutron groups at resonance provides closer inspection of this effect. Figure 9 shows the temperature dependence of the phonons in E_g symmetry in $(KBr)_{0.965}(KCN)_{0.035}$ at the resonance frequency, which is now shifted to energies slightly above 2 meV. Again, there are only minor effects in energy and linewidth in passing T_F. A more detailed investigation of this crystal has already been published in Ref. 11. Finally, constant-$\vec{Q}$ scans in $(KBr)_{0.84}(KCN)_{0.16}$ are given in Figs. 10 and 11 in the paraelastic and glass states, respectively. Obviously the damping of the coupled modes is now increased compared to the lower concentrations, although a double-peak structure is still visible. The resonant frequency is shifted to 4 meV and is again unaffected by the onset of freezing. After a rough inspection of the resonant frequencies and the linewidths of the scattered-neutron groups in E_g symmetry, we can summarize our results as follows.

(i) The energy of the molecular excitation depends sensitively on the concentration x.

(ii) Neither the excitation energies nor the linewidths are noticeably changed by the freezing process into the glass state. This is contradictory to the relaxational models with an Arrhenius-type behavior of the relaxation times, which predict small linewidths at the lowest temperatures in the orientational glass state. However, one might argue that the interaction in E_g symmetry is weak compared to the rotation-translation coupling in T_{2g} symmetry,[18] and therefore the dominant effects are expected to show up in T_{2g}-symmetry modes.

C. Coupled modes in T_{2g} symmetry

In the mixed crystal with a concentration $x=0.008$ the neutron groups at wave vectors $q/q_{zB} \geq 0.6$ show no anomalies and their energies are temperature independent within the error bars. However, distinct effects are observed at smaller wave vectors. For phonon wave vectors $q/q_{zB} \leq 0.05$ the inelastically-scattered-neutron groups in the [100] T_y branch pass through a minimum at 10 K, as shown in Fig. 5. At temperatures $T \leq 2$ K, a coupled-mode behavior becomes apparent with a resonant frequency of approximately 0.3 meV. Constant-$\vec{Q}$ scans at 2 K in the wave-vector region of the strongest interaction are shown in Fig. 12. The rather unusual temperature dependence of the rotation-translation hybridization is documented in Fig. 13. The double-peak structure at 1.8 K is changed into a single broad peak of 4.2 K, indicating purely relaxational-type behavior. A rough inspection also shows the frequency shift of the scattered-neutron groups with the lowest frequency occurring around 11 K.

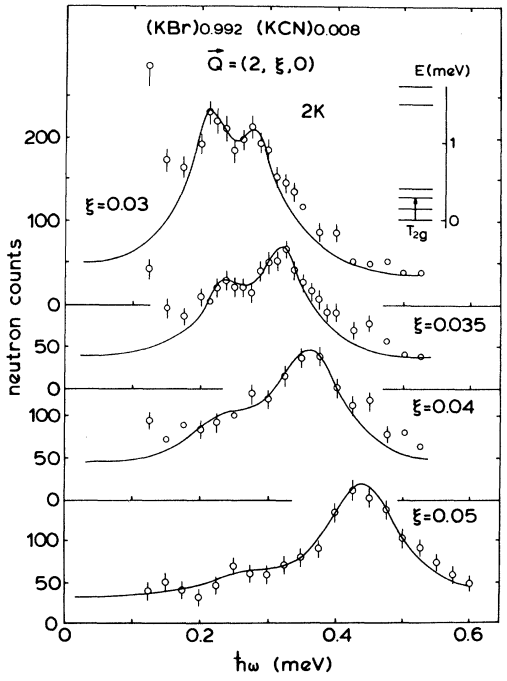

FIG. 12. Low-temperature neutron-scattering line shapes in T_{2g} symmetry ($x=0.008$ sample) for various momentum transfers near the mode-crossing region. The solid lines are calculated from the Silverman model using a level scheme as shown in the inset.

For $(KBr)_{0.84}(KCN)_{0.16}$ we did not detect neutron groups with a double-peak structure indicating a hybridization of the [100] T_y phonon branch with a tunneling or a librational excitation. Instead, we observed anomalously

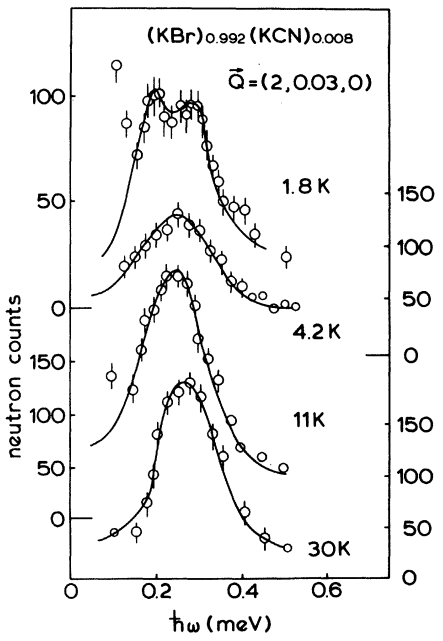

FIG. 13. Temperature dependence of the neutron-scattering line shape at constant momentum transfer ($x=0.008$ sample) in the resonance region. The solid lines are fits using the theoretical model.

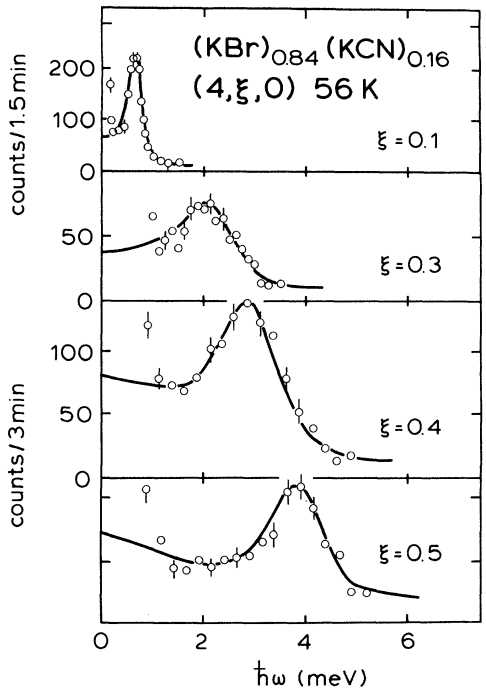

FIG. 14. Neutron-scattering line shapes in T_{2g} symmetry at 10 K for different momentum transfers ($x=0.16$ sample).

broadened groups at energies of around 2 to 3 meV (Figs. 14 and 15). This can be explained by a coupling of T_{2g} phonons to overdamped rotational modes. As outlined in Sec. II, in this case we expect a pure relaxational-type behavior where the strongest interactions appear just at

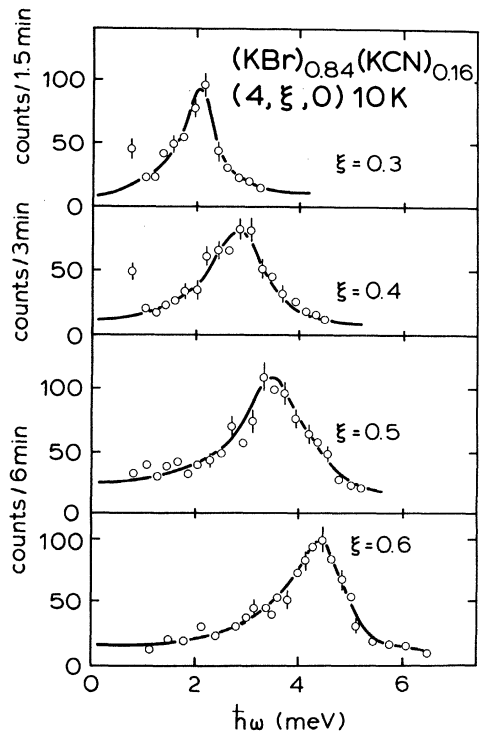

FIG. 15. Neutron-scattering line shapes in T_{2g} symmetry at 10 K for different momentum transfers ($x=0.16$ sample).

frequencies $\omega\tau=1$, where τ is the relaxation time of the CN^- ions. The data suggest that τ is unaffected in passing the freezing temperature T_F. A detailed experimental investigation has already been published.[11] Summarizing the results in T_{2g} symmetry we find the following.

(i) In $(KBr)_{0.992}(KCN)_{0.008}$, a pure relaxational model can explain the experimental results down to 4 K. The phonon frequencies at fixed wave vectors pass through a minimum at T_F and no double-peak structure of the scattered-neutron groups is apparent, but at 2 K a clear hybridization of the [100] T_y phonon mode with a rotational excitation is found.

(ii) In $(KBr)_{0.84}(KCN)_{0.16}$, a relaxational-type behavior is seen at all temperatures. Surprisingly, it seems that the relaxation time τ is temperature independent, which again contradicts the predictions of an Arrhenius law. The short relaxation times which make the tunneling transitions unobservable at all temperatures could be due to the strongly increased defect interactions for $x=0.16$.

V. ANALYSIS OF THE EXPERIMENTAL RESULTS

To find a more quantitative description of the behavior of the coupled rotational-translational modes at the transition from the paraelastic to the structural glass state, we analyzed all the measured neutron line shapes using the formalism outlined in Sec. II. In these fitting procedures the relevant parameters were the uncoupled "background" elastic constant C_0, the level splitting Δ, the line broadening Γ of the rotational excitations, and the rotation-translation coupling $T_S=xg^2$. Here, we assumed, for long wavelengths, $G^2=g^2\omega_0^2(\vec{q})$.

In E_g symmetry we found at all concentrations investigated, namely $x=0.008$, 0.035, and 0.16, a mode-mode–coupling behavior in the limit $\Delta\gg\Gamma$. The parameters as found in the analysis are listed in Table II. The quality of the fits is shown as solid lines in Figs. 6–11. The relevant quantitative results are as follows.

(i) Both the level separation Δ and the linewidth Γ are strongly concentration dependent. Δ increases from 1.8 meV at $x=0.008$ to 4 meV at $x=0.16$. This increase in the energy separation might be due to modifications in the crystal-field parameters K and ϕ in the nomenclature of Beyeler.[25] The linewidth Γ, measured at the lowest temperatures, increases from 0.3 meV ($x=0.008$) to 1.3 meV ($x=0.16$). It seems that this effect is an inhomogeneous broadening due to concentration effects. At this point we note that the single-ion model used in the present analysis hides several effects in the parameter Γ, namely (1) an Arrhenius-type lifetime effect due to thermal activation across the hindering barriers of a single-ion Devonshire potential, (2) the static T-independent distributions of the potential due to the local chemical environment, and (3) a time-dependent modulation of the potential due to molecular motions of interacting neighboring CN^- ions. The inhomogeneous broadening mentioned above is solely due to effect (2).

(ii) The level separation Δ and the linewidth Γ of the molecular excitation show only minor effects at the transition from the paraelastic to the orientational glass state. Only in the $x=0.16$ sample does a reduction of Γ by 30% with decreasing temperatures become apparent. This again shows that the static T-independent distribution of the potential is dominant in the linewidth of the molecular transition in E_g symmetry. The crystal-field parameters K and ϕ remain the same across T_F.

(iii) If we analyze the scattered-neutron groups by assuming a temperature dependence of the two-level model in the limit $\Delta\gg\Gamma$ according to Eq. (2), there is a decrease in the coupling parameter $T_S=xg^2$ in the orientational glass state. It is worthwhile to note that the rotation-translation coupling as determined from these neutron experiments agree well with ultrasonic results in the paraelastic and glassy states.[14,18] The value of g^2 can be directly compared to the coupling constant in E_g symmetry in pure KCN determined from ultrasonic experiments. Here, Rehwald *et al.*[30] found a value of $g^2=112$ K, which fits in nicely to the results listed in Table II.

In T_{2g} symmetry the analysis of the inelastically-scattered-neutron line shapes is much more complicated. In $(KBr)_{0.992}(KN)_{0.008}$ the only relevant interaction was found at 0.25 meV. The results for $T\leq 2$ K could be analyzed in terms of coupled modes according to Eq. (2) with $\Delta\gg\Gamma$. Surprisingly, these results are almost indentical with those of Rowe *et al.*[5] on a crystal with a CN concentration 20 times lower. Upon increasing the tem-

TABLE II. Parameters determined from the fits of the Silverman model to the observed neutron line shapes along [110] T_{xy} (E_g symmetry). (nd denotes "not determined.")

x	$T_F(\omega\sim$THz) (K)	T (K)	C_0 (10^{10} dyn/cm^2)	Δ (meV)	Γ (meV)	$T_S=xg^2$ (K)	g^2 (K)
0.008	10.0	2.0	19.5	1.75±0.05	0.30±0.02	0.9±0.1	113.0±30.0
		4.8	18.8	1.73±0.05	0.29±0.02	0.9±0.1	113.0±30.0
		15.0	19.8	1.93±0.05	0.33±0.02	1.1±0.1	138.0±30.0
		30.0	20.0	1.95±0.05	0.31±0.02	1.2±0.15	150.0±43.0
0.035	nd	6.0	15.8	2.40±0.1	0.6 ±0.05	2.5±0.1	71.0±15.0
		35.0	16.0	2.50±0.1	0.65±0.05	4.0±0.15	114.0±24.0
		60.0	16.0	2.50±0.1	0.65±0.05	4.0±0.15	114.0±24.0
0.16	55.0	8.5	16.3	4.0 ±0.1	1.3 ±0.1	5.0±0.5	31.0± 5.0
		58.0	16.0	3.8 ±0.1	1.8 ±0.1	17.0±0.5	106.0±12.0

TABLE III. Parameters determined by fitting of the Silverman model to the neutron line shapes observed in the [100] T_y branch (T_{2g} symmetry).

x	T_F (K)	T (K)	C_0 (10^{10} dyn/cm^{-2})	Δ (meV)	Γ (meV)	$T_S=xg^2$ (K)	g^2 (K)
0.008	10	1.8	5.0±0.1	0.24±0.02	0.025±0.005	0.19±0.02	27.5± 6.0
		2.0	5.2±0.1	0.26±0.02	0.030±0.005	0.18±0.02	22.5± 6.0
		4.5	5.0±0.1	~0.3	0.200±0.10	0.90±0.05	112.5±23.0
		8.0	5.0±0.1	$\lesssim\Gamma$	0.250±0.10	1.20±0.15	150.0±40.0
0.16	55	10.0	5.1±0.1	$\lesssim\Gamma$	3.0 ±0.2	4.5 ±0.5	28.0± 5.0
		56.0	5.1±0.1	$\lesssim\Gamma$	2.7 ±0.2	25.0 ±2.0	156.0±25.0
		80.0	5.1±0.1	$\lesssim\Gamma$	2.8 ±0.2	28.0 ±2.0	175.0±25.0

peratures we found a strong increase in the linewidth Γ, and for temperatures $T\geq 4.5$ K the relaxational limit ($\Delta\lesssim\Gamma$) was adequate. The parameters as determined from the fits of the pseudospin model to the experimental line shapes are given in Table III. Above the freezing temperature ($T>10$ K) we calculated T_S only according to the softening of the phonon frequencies, and found a constant rotation-translation coupling $T_S\simeq 1.2$ K in the paraelastic phase. Extrapolated to pure KCN, this yields a coupling constant $g^2=150$ K compared to a value of 151 K as deduced from the elastic data in KCN.[18,30] The relevant results in $(KBr)_{0.0992}(KCN)_{0.008}$ in T_g symmetry are shown in Fig. 16. T_S is temperature independent for $T>T_F$, while below T_F a strong reduction of the coupling constant could be detected.

The inverse lifetime Γ of the tunneling transition varies—within experimental error—linearly with temperature. One expects this behavior for a thermal modulation of the tunneling barrier, while an Arrhenius-type behavior would be the case when the lifetime of the tunneling states are limited by thermal activation across the barrier or by excitations to librational states. These results contradict previous results, where the frequency dependence of the freezing temperatures was explained by an Arrhenius-type behavior of the inverse lifetime.[15,16,19] The complex behavior of the coupled modes in T_{2g} symmetry in $(KBr)_{0.992}(KCN)_{0.008}$ results from a crossover from fast ($\omega\tau<1$) to slow relaxation ($\omega\tau>1$), and a crossover from a coupled-mode behavior in the limit $\Delta\gg\Gamma$ to a purely relaxational behavior ($\Delta<\Gamma$). We presume that both crossovers take place at $T\sim 10$ K accidentally.

To describe the experimental data in $(KBr)_{0.84}(KCN)_{0.16}$ we used the Silverman model in the relaxational limit according to Eq. (6). The results are shown as solid lines in Figs. 14 and 15. The fitting parameters are listed in Table III. In this crystal with a high CN concentration the linewidth is temperature independent and essentially the same in the glassy and paraelastic states, a behavior that is very different from the findings in $(KBr)_{0.992}(KCN)_{0.008}$. This T-dependent behavior of the linewidth of the molecular excitation can be described by effect (2) as mentioned above: At high

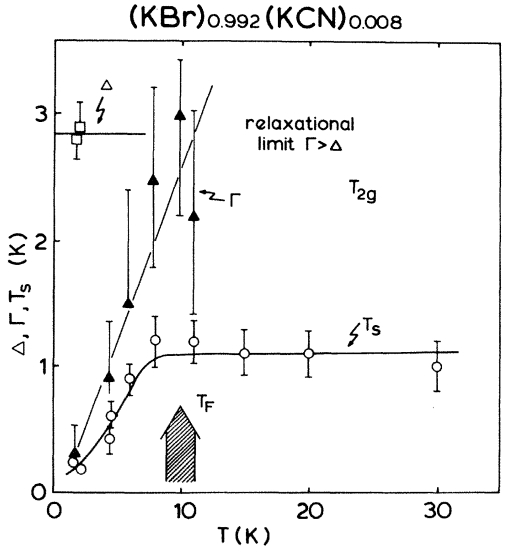

FIG. 16. Temperature dependence of the level separation Δ (□), the linewidths Γ (▲), and the coupling constant T_S (○) of the molecular susceptibility as measured in T_{2g} symmetry in the $x=0.008$ sample. The solid lines guide the eye. The freezing temperature is indicated by the arrow.

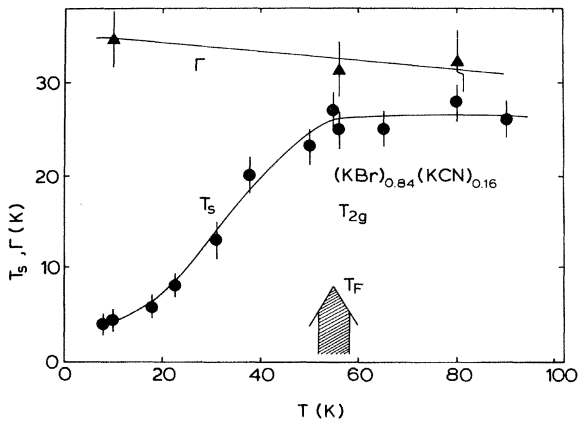

FIG. 17. Temperature dependence of the linewidth Γ (▲) and the coupling constant T_S (●) of the molecular susceptibility as measured in T_{2g} symmetry in the $x=0.16$ sample. The solid lines guide the eye. The freezing temperature is indicated by the arrow.

CN concentration, the local chemical environment yields broad static distributions of the hindering potential which dominate the linewidth Γ. The rotation-translation coupling is again drastically reduced in the structural glass state. A summary of the temperature dependence of T_S and Γ in $(KBr)_{0.84}(KCN)_{0.16}$ is shown in Fig. 17.

VI. DISCUSSION

We want to emphasize that the evaluation of the neutron data is based on a model which couples the acoustic phonons to an extremely simplified molecular susceptibility. In particular, this susceptibility is a single-particle response function. In our type of analysis, multiparticle effects, which exist definitively between the CN^- ions, can appear artificially only in the single-particle parameters Δ, Γ, and $T_S = xg^2$.

In E_g symmetry a molecular excitation is observed at an energy of about 1.8 meV in $(KBr)_{0.992}(KCN)_{0.008}$. From theoretical work on the energy states of a CN^- ion in a cubic Devonshire potential (see Fig. 1), and from neutron measurements on CN impurities in KBr (Ref. 5) and KCl (Ref. 8), it is presumably correct to regard this excitation from the tunnel-split ground state to an excited E_g state as a libration around the $\langle 111 \rangle$ easy axes of the potential. Higher concentrations lead to higher values of the librational energy (Table II). This trend may be either due to deeper potential wells or to a coupling between the CN dumbbells.

Obviously, the molecular excitation in T_{2g} symmetry is a transition within the tunnel-split ground state. It describes reorientational motion of CN^- ions between equivalent $\langle 111 \rangle$ directions in the crystal. Asymmetrical effects in the potential due to a different local chemical environment show up as linewidth effects.

If we now consider this different character of the two excitations—the T_{2g} tunneling transition triggers reorientations, whereas the E_g librations maintain the alignment of the molecule—we easily gain insight into the glass-formation process. If the freezing temperature signals the onset of the blocking of CN^- ions in clusters with random pattern of $\langle 111 \rangle$ orientations, it is likely that the number of single-ion tunneling states is highly reduced and restricted to individual molecules which are not firmly incorporated into the clusters. However, librational modes should still be possible within the clusters. Their oscillator strength is reduced only in favor of new collective excitations of the frozen-in clusters. From our experimental results we conclude that these new cluster modes are effectively decoupled from the lattice strains. At the lowest temperature only some isolated dumbbells can tunnel, while the majority are blocked in clusters with little direct effect on the phonons. This effective reduction of the concentration explains the similarity of our results to those of Rowe *et al.*[5] in a crystal with a concentration 20 times lower.

The present results give a clear understanding of the structural glass transition in $(KBr)_{1-x}(KCN)_x$ and they are of importance to the physics of spin-glasses in general:[31] At the freezing temperature, strain-mediated interactions overcome, in certain regions of the crystal with the strongest local fields, thermal-activation processes of the single-ion molecules, leading to the blocking of some of the CN dumbbells in clusters of pairs, triplets, etc., without destroying the overall cubic symmetry of the crystal. The rest of the molecular system remains as isolated CN^- ions with relaxation times appropriate for the single-ion case. The clusters grow with decreasing temperatures. The maximum in the quadrupolar susceptibility occurs through a competition between the setup of local order and a T^{-1} Curie law of the free ions. The cluster-formation process reduces the number of single-ion tunneling states which are strongly coupled to the lattice in favor of new, only weakly coupled collective modes representing cluster-reorientation processes. The different clusters give a broad distribution of low-energy excitations which have little direct effect on the ultrasonic properties on the dynamic structure factor in an inelastic neutron scattering experiment, but they will contribute in calorimetric experiments depending on the timescale employed. Similar low-lying energy states are believed to be important in the low-temperature properties of "real" glasses as proposed by Anderson *et al.*[32] and by Phillips.[33]

In conclusion, the present experimental results can be explained with a structural glass state in K(Br,CN) which is characterized by the formation of clusters of orientationally correlated CN^- ions and which results in a drastic reduction of the number of phonon-induced tunneling states, thus making molecular reorientations very improbable. This leads to a metastable phase at low temperatures with extremely long relaxation times.

ACKNOWLEDGMENTS

We acknowledge helpful comments on the formation of the glass state by J. M. Rowe. One of us (A.L.) would like to thank the members of the Physics Department at Risø National Laboratory for their kind hospitality.

[1]F. Lüty, Phys. Rev. B 10, 3677 (1974).
[2]F. Lüty, in *Defects in Insulating Crystals,* edited by V. M. Turkwitch and K. K. Svats (Springer, Berlin, 1981).
[3]F. Holuj and F. Bridges, Phys. Rev. B 20, 3578 (1979).
[4]R. Windheim, Solid State Commun. 18, 1183 (1976).
[5]J. M. Rowe, J. J. Rush, S. M. Shapiro, D. G. Hinks, and S. Susman, Phys. Rev. B 21, 4863 (1980).
[6]J. M. Rowe, J. J. Rush, J. W. Chesser, K. H. Michel, and J. Naudts, Phys. Rev. Lett. 40, 455 (1978).
[7]A. Loidl, K. Knorr, J. Daubert, W. Dultz, and W. J. Fitzgerald, Z. Phys. B 38, 153 (1980).
[8]D. Walton, H. A. Mook, and R. M. Nicklow, Phys. Rev. Lett. 33, 412 (1974).
[9]R. M. Nicklow, W. P. Crummett, M. Mostoller, and R. F. Wood, Phys. Rev. B 22, 3039 (1980).
[10]R. F. Wood and M. Mostoller, Phys. Rev. Lett. 39, 819 (1977).
[11]A. Loidl, R. Feile, K. Knorr, B. Renker, J. Daubert, D.

Durand, and J. B. Suck, Z. Phys. B 38, 253 (1980).
[12]D. Durand and F. Lüty, Ferroelectrics 16, 205 (1977); D. Durand (unpublished).
[13]J. M. Rowe, J. J., Rush, D. J. Hinks, and S. Susman, Phys. Rev. Lett. 43, 1158 (1979).
[14]A. Loidl, R. Feile, and K. Knorr, Z. Phys. B 42, 143 (1981).
[15]A. Loidl, R. Feile, and K. Knorr, Phys. Rev. Lett. 48, 1263 (1982).
[16]S. Bhattacharya, S. R. Nagel, C. Fleishman, and S. Susman, Phys. Rev. Lett. 48, 1267 (1982).
[17]C. W. Garland, J. Z. Kwiecien, and J. C. Damien, Phys. Rev. B 25, 5818 (1982).
[18]R. Feile, A. Loidl, and K. Knorr, Phys. Rev. B 26, 6875 (1982).
[19]K. Knorr and A. Loidl, Z. Phys. B 46, 219 (1982).
[20]F. Lüty and J. Ortiz-Lopez, Phys. Rev. Lett. 50, 1289 (1983).
[21]K. H. Michel and J. M. Rowe, Phys. Rev. B 22, 1417 (1980).
[22]B. Fischer and M. W. Klein, Phys. Rev. Lett. 43, 289 (1979).
[23]D. G. Bounds, M. L. Klein, I. R. McDonald, and Y. O. Ozaki, Mol. Phys. 47, 629 (1982).
[24]A. F. Devonshire, Proc. R. Soc. London, Ser. A 153, 601 (1936).
[25]H. U. Beyeler, Phys. Status Solidi 52, 419 (1972).
[26]R. C. Casella, Phys. Rev. B 20, 5318 (1979).
[27]K. H. Michel, J. Naudts, and B. De Raedt, Phys. Rev. B 18, 648 (1978); B. De Raedt and K. H. Michel, Phys. Rev. B 19, 767 (1979).
[28]B. D. Silverman, Phys. Rev. Lett. 25, 107 (1970).
[29]Y. Yamada, Ferroelectrics 16, 49 (1977).
[30]W. Rehwald, J. R. Sandercock, and M. Rossinelli, Phys. Status Solidi A 42, 699 (1977).
[31]U. T. Höchli, Phys. Rev. Lett. 48, 1494 (1982).
[32]P. W. Anderson, B. I. Halperin, and C. M. Varma, Philos. Mag. 25, 1 (1972).
[33]W. A. Phillips, J. Low Temp. Phys. 7, 351 (1972).